Society for Space Education Research & Development

EDUCATE - INSPIRE - INNOVATE

SSERD

FW-LB

Aerodynamic Study of HL-20 Design Modification

Redefining the future of space travel

Team FW-LB

Supervised by

Mr. Pavan Kumar
External Guide, SSERD

Mr.Sujay Sreedhar
Internal Guide & Chairman, SSERD

August 06th, 2020

A dissertion submitted in partial fulfilment of the requirements for the certification of SSERD.

Declaration

We, **Mr. Apurva Majumdar** R17ME033 of REVA University, **Mr. Mridul Agarwal** 180010034 and **Mr. M Vishnu Sankar** 18B030013 of Indian Institute of Technology Bombay, **Mr. Thejas K. V.** 17ETAS012062, **Mr. Maaz Ahmed Shariff** 17ETAS012023 and **Miss. Anshoo Mehra** 17ETAS012004 of M. S. Ramaiah University of Applied Sciences, **Mr. Nikhil S N** 1DS17AE029, **Miss. Preethi S** 1DS17AE033, **Miss. S Akshaya** 1DS17AE059, **Miss. Vinutha G** 1DS17AE056 and **Miss. Isha G** 1DS17AE060 of Dayananda Sagar College of Engineering, **Mr. Soumitra Manish Dodkey** 18103086 of Hindustan Institute Of Technology and Science, **Mr. Mihir Rai** AE18B114 Indian Institute of Technology Madras, **Mr. Nagachandra N** PES1201700570 of PES University Bengaluru, **Miss. Uttkarsha Gupta** AIT17BEAE060 Acharya Institute of Technology Bangalore, **Mr. Shivam Suri** 17BAS1174 of Chandigarh University, **Mr. V Kabbilaash Kumar** UR16AE052 of Karunya University, **Mr. NOUFAL R** ACE18AN020 of ACE College of Engineering TVM, **Mr. Vijay S** 17101105 of Hindusthan College of Engineering and Technology, **Mr. Atharva** 17112017 of Indian Institute of Technology- Roorkee and **Miss. Manabi Maity**, hereby declare that, this research internship work entitled **"Aerodynamic Study of HL-20 Design Modification"** has been carried out by us under the guidance of **Mr. Sujay Sreedhar** who is the Co-founder and Chairman of Space Education Research and Development and **Mr. Pavan Kumar** who is pursuing PhD in Partial Differential Equation (Variational Formulation) for mechanics problems at IMT School for Advanced Studies.

Acknowledgements

Before introducing our research internship work, we would like to thank the people without whom the success of this work would have been impossible. We express our deepest gratitude and indebtedness to Mr. Sujay Sreedhar who is the Co-Founder and Chairman of Society for Space Education Research and Development and Miss. Nikhitha C who is also the Co-founder Chief Executive Officer of Society for Space Education Research and Development. The organization gave us the opportunity during a COVID-19 pandemic to allow students from different parts of India to come and work together virtually.

We would like to thank Mr. Sujay Sreeddhar yet again for taking up the role of our internal guide and constantly monitoring our work. We extend our gratitude to Mr. Pavan Kumar for being our external guide and sharing some wonderful insights in our research process. Their constant support and encouragement was instrumental in completion of this research work. The guidance that we received from them helped us at each step in successfully completing our work on time.

We feel short of words to express our heartfelt thanks to the entire SSERD team and to all our family members and friends and all those who have directly or indirectly helped us during the course of this Internship.

Abstract

Lifting Body Re-entry Vehicle configuration is one of the most promising approaches for developing a reusable re-entry vehicle. The combination of lifting re-entry and ballistic re-entry enables these vehicles to achieve deceleration values optimum for crewed re-entry. It also provides the vehicle an increased accuracy in landing, minimized heating rates and fair control over the maneuvers. The optimization of the vehicle body shape to achieve desired lift to drag ratio and low ballistic coefficient is one of the prime focus of research on these vehicles. The diameter of launch vehicles imposes a constraint on the width of the re-entry vehicle design which directly affects the planform area of the re-entry vehicle. HL-20 PLS vehicle is a lifting body configuration developed by NASA Langley Research Centre in the 1990s with an intent to achieve frequent manned orbital missions. This study focuses on the aerodynamic effects of incorporating a retractable wing extension on the HL-20 PLS design. The simulation results indicate an improved lift to drag ratio performance at lower angles of attack for the modified HL-20 PLS design with wing extensions. The modified design is also observed to showcase an early stall character in comparison with the original design.

Contents

List of Figures

List of Abbreviations

NASA National Aeronautics and Space Administration

ACRC Assured Crew Return Capability

PLS Personnel Launch System

L/D Lift by Drag ratio

B.C. Ballistic Coefficient

M Mach Number

CFD Computational Fluid Dynamics

g Gravitational acceleration of Earth

C$_D$ Coefficient of Drag

C$_L$ Coefficient of Lift

CATIA Computer Aided Three dimensional Interactive Application

igs Initial Graphics Exchange Specification

ANSYS Analysis System

AOA Angle of Attack

1

Introduction

Flying Wings and Lifting Body configurations are quite often viewed as unconventional aircraft concepts. On the contrary, these configurations are more popular in the designing of modern reentry vehicles. In a broad sense, the Flying Wing configuration can be defined as a vehicle that accommodates all of its body within the structure frame of a wing profile. On a similar note, a Lifting Body can be defined as a vehicle that is aerodynamically shaped to generate lift performance similar to that of a wing. Lifting Body configurations are usually characterized with small wing sections or no wings in their design.

The flying wing emerges to be one of the most assuring configurations when it comes to the designing of sub-orbital flights. This configuration covers a range of vehicle concepts like blended wing-body, C-wing, tailless aircraft, etc. Fuel savings and lower pollution rate are the foremost merits of a flying wing configuration. Since the engines can be mounted above the wing and the aircraft does not require complex high lift devices, this configuration results in a much quieter airplane.

A lifting body is essentially a wingless vehicle that flies due to the lift generated by the shape of its fuselage. The lifting-body concept was a radical departure from the aerodynamics of conventional winged aircraft. However, the most logical method for generating lift is through wings, but wings do create issues because they need to be extremely strong to handle the aerodynamic and the thermal stresses at hypersonic speeds during re-entry phase.

Majority of the re-entry vehicle designs in the 20th century used the ballistic re-entry approach with a conical capsule design. Despite their success, they were limited by the requirements of large-area landing and diminished re-entry control. The concept of lifting body reentry vehicles evolved during the early 1960s at NASA. They were mainly influenced by the Burnelli designs of lifting fuselages. Some notable early lifting body designs include M2-F2, HL-10 and X-24. HL-20 happens to be one such lifting body design developed by the Langley Research Center at NASA. It was developed as a part of two NASA programs, Assured Crew Return Capability ACRC Program and the Personnel Launch System (PLS) program, with a concept for manned orbital missions.

The overall design of the HL-20 PLS concept has incorporated the deterrent from the operation of the Space Shuttle. Vehicle subsystems are located close to the exterior of the vehicle and removable panels are provided for easy access to these subsystems for quick vehicle maintenance and turnaround. Overall, HL-20 PLS vehicle processing is expected to be substantially less than for the Space Shuttle orbiter. This vehicle would be launched into the orbit by a booster rocket or carried within the payload bay of the space shuttle orbiter. The vehicle would then deorbit by using an on-board propulsion system and perform a nose first re-entry and horizontal, possibly unpowered landing. It is designed to carry up to 10 people and very little cargo. The test results indicate the vehicle has a trimmed maximum hypersonic L/D of about 1.4. At subsonic speeds the vehicle has longitudinal trim at close to maximum L/D and a subsonic L/D of about 4.2.

This reusable vehicle, designated the HL-20, has been designed for safe and reliable operations; improved operability, maintainability and affordability; and reduced life-cycle costs associated with placing people in orbit. The results of the human factors studies have shown where improvements in the baseline HL-20 design are desirable. These improvements will have little impact on overall vehicle shape or aerodynamic performance.

The ballistic coefficient (B.C.) describes how air resistance slows a projectile in flight. Low ballistic coefficients of the spacecraft will be effective in reducing the heat rate on the surface of the spacecraft. Therefore, in this research work an attempt has been made

to reduce ballistic coefficient of the HL-20 design with the addition of retractable wing extensions.

1.1 | Motivation

The three crucial parameters affecting the sub-orbital and orbital space flights are deceleration of the spacecraft, heating rates during the descent and safe landing with accuracy. For unmanned space flights, the deceleration rate is limited by the structural loading that a spacecraft can take. However, human crew space exploration missions add an additional constraint on the deceleration limiting the maximum 'g' load around 6-7 g's. For a safe re-entry, the spacecraft must be ensured to remain in the re-entry corridor, ensuring the right flight velocity and drag conditions. If the entry angle is too steep the spacecraft would cross the undershoot boundary leading to rapid deceleration and adverse heating.

Spacecrafts with low-ballistic coefficients are much efficient in minimizing the heating rate on the spacecraft surface and ensuring optimum deceleration. The ballistic coefficient is inversely proportional to the cross-sectional area facing the flow direction. The width of spacecrafts designed for suborbital and orbital flights are constrained by the diameter of the launch-vehicle. The incorporation of extendable surfaces helps in overcoming the limitation of this constraint. During reentry, this additional surface area will help in minimizing the ballistic coefficient and increasing the lift generation.

1.2 | Aims and Objectives

During the initial survey, the performance parameters of SpaceShip Two developed by Virgin-Galactic and Dream Chaser developed by Sierra Nevada Corporation were found to be promising for suborbital and orbital flights. SpaceShip Two employs a unique feather configuration to increase the drag for deceleration during re-entry. But it suffers in achieving directional stability at low supersonic speeds. Dream Chaser is a lifting body configuration which uses the body lift generated to decelerate the space-

craft. It is a successor of HL-20 Personnel Launch System developed by NASA and shares very close similarity with respect to design. The flat belly surface in both the designs make them the best suitable vehicle for incorporating an extendable wing surface. This project aims to study the aerodynamic effects of incorporating a retractable wing extension to the HL-20 design in comparison with the original configuration. The wing extension is intended to provide a larger surface area during re-entry, thereby increasing the lift and reducing the ballistic coefficient of the spacecraft.

2

Literature Survey

Soumyo Dutta et al. (12) have investigated the design challenges in implementing entry systems to Venus with shallow flight path angles and low ballistic coefficient. The possibility of using a deployable aeroshell during Venus entry to increase the wetted area and its effect on achieving a better trajectory is discussed.

Jeffrey S. Robinson et al. (11) have presented an investigation related to trajectory planning for crewed re-entry vehicles along with associated aero-heating environments. The re-entry data related to the Apollo Command Module is used to serve as a baseline for investigation. It presents methods used for identifying trajectories suitable for ablative systems and reusable systems. These methods include the selection of a reasonable range of initial velocity, ballistic coefficients and initial flight path angles to generate the trajectories.

G. M. Ware et al. (9) have studied the aerodynamic characteristics of HL-20 configuration and conclude about the lateral and longitudinal stability of the design in test Mach number range from 10 to 0.2. The study also presents the modifications to the outboard fins into an airfoil shape and the associated effects on improved L/D ratio.

Yongyuan Li et al. (8) have presented the use of Genetic Algorithm for optimizing the aerodynamic shape of a lifting body. It uses the shape parameters of existing lifting body designs as design variables to optimize the aerodynamic characters.

Dan Almosnino (7) has presented a study on the use of Euler-Adjoint solver for studying the aerodynamic characteristics of HL-20 for Mach number ranging from M=0.3 to

M=20. The study makes use of a 7% scale model for running the simulation and presents the computational considerations specific to the solver used.

K. James Weilmuenster et al. (5) have investigated the solution techniques for CFD analysis of HL-20 configuration at hypersonic conditions. The results indicate the negligible real-gas effects on the aerodynamic characters of the vehicle at these conditions. The results of surface heating were found to match closely with those obtained from Navier-Stokes solutions.

Zachary R. Putnam et al. (4) have presented a study on the feasibility of flying HL-20 without a steady-state body flap deflection.

R. Dale Reed (16) has recorded the early history and development of Lifting Body designs in the book 'Wingless Flight'. It explores the various factors and design considerations that have coursed the lifting body designs for suborbital flights and space flights.

Richard M. Wood et al. (1) have presented a detailed study on the various classes of lifting vehicles including flying wing and lifting body designs. The paper describes the relationships between these classes and also marks the importance of some of the influential designs belonging to these lifting vehicle classes.

B. Spencer et al. (2) have investigated into providing Personnel Launch System vehicle that is inherently stable from the re-entry phase to landing. It also looks into the improvement of aerodynamic performance of HL-20 in subsonic regimes by making few modifications into the original design. The paper also presents the cross-sectional dimensions of the original HL-20 7% scale model along the longitudinal axis. This data is used in our study to prepare the HL-20 model for simulation.

3

Methodology

The ballistic coefficient of a re-entry vehicle depends on the mass, drag coefficient and the cross-sectional area of the vehicle in the direction of velocity. It is given by the formula

$$B.C. = \frac{M}{C_D * A} \tag{3.1}$$

where,

$B.C.$ – Ballistic Coefficient

M – Mass of the spacecraft

C_D – Drag Coefficient

A – Cross-sectional area in the direction of velocity

The mass of the spacecraft is less ideal to be used for the control of ballistic coefficient during re-entry. In lifting body designs, the drag coefficient and the cross-sectional area are adjusted to obtain a desired ballistic coefficient by controlling the angle of attack of the vehicle. In order to achieve a lower ballistic coefficient, the angle of attack has to be increased to increase the effective area in the direction of velocity. An increased angle of attack can severely affect the lift generation beyond the stall angle, thereby setting up a limitation. The use of extendable wings can ensure the achievement of a low ballistic coefficient at a relatively lower angle of attack.

The aerodynamic performances of the original HL-20 configuration from experimental studies for Mach numbers ranging from 0.3 to 10 were studied. In order to demonstrate

the feasibility of using this vehicle for sub-orbital flight space tourism, the study was focused on the descent phase from 100 km to 60 km altitude. A study was carried out to explore the mathematical models for Computational Fluid Dynamic simulations that were feasible with the aerodynamic and thermodynamic conditions at those altitudes. Due to computational limitations, it was decided to study the aerodynamic characters at a Mach Number of 4 with free-stream conditions matching that of 60 km altitude for both the original and the modified HL-20 configurations. The range of angle of attack for the simulation was set from -5 degree to 35 degree. The obtained lift and drag coefficients were then used to draw a comparison between the variation in these parameters for both the models.

4

Design & Analysis

The modelling of the HL-20 vehicle was done using the CATIA V5 modelling tool. The essential cross-section dimensions for modelling were obtained from a journal paper presented by B. Spencer et al. The paper had presented the dimensions of a 7% scale model. This was scaled up to obtain the original dimensions of the HL-20 vehicle. A hybrid design environment is used on CATIA V5 software to enable the development of complex surfaces. The design process involved the construction of a wireframe model from the computed dimensions, generation of surfaces from the curves and conversion of surface model into a solid model.

Construction of Wireframe Model: The wireframe and surface modelling environment is used initially to generate a wireframe model. The profile of the HL-20 about its symmetric plane along the longitudinal axis was constructed. Nine cross sectional planes at locations 0.05, 0.14, 0.25, 0.34, 0.45, 0.60, 0.75, 0.90 and 1.0, expressed as fractions of total length from the nose of the vehicle were constructed. The contour of the vehicle as projected on these planes were constructed by identifying few critical contour points. The completed wireframe model is then checked for any mismatched point while generating the curves.

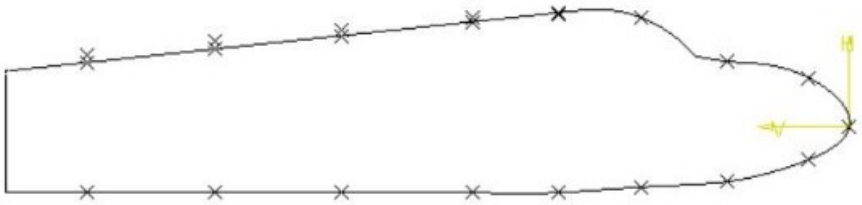

Figure 4.1: Profile on Symmetric Plane along Longitudinal Axis

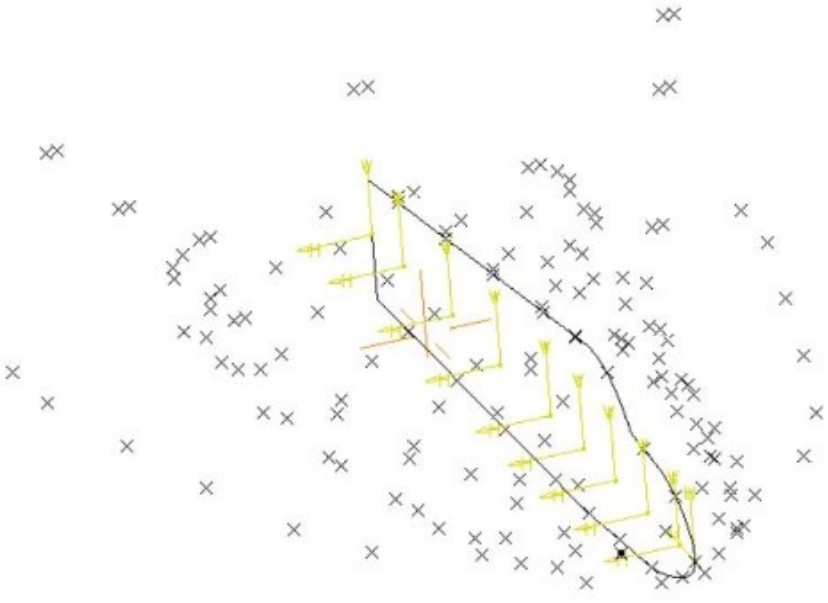

Figure 4.2: Construction of critical contour points for generating profile curves

Development of Solid Model: The closed curves in the wireframe model are then used to generate surfaces. The selection of closed curves was carefully done so as to maintain continuous adjoining surfaces throughout the model. The surfaces so developed are then stitched together to enclose one single model. In the part design environment, the stitched surface model is converted into solid model. The completed model is then exported to igs format.

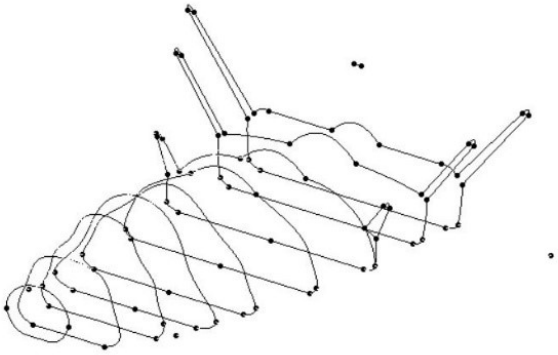

Figure 4.3: Contour projections developed on the nine cross-sectional planes about the Longitudinal axis

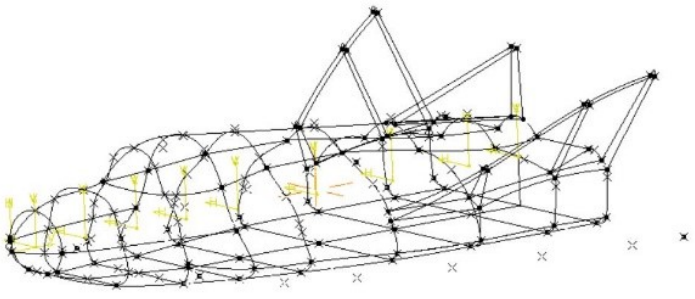

Figure 4.4: Completed Wireframe Model

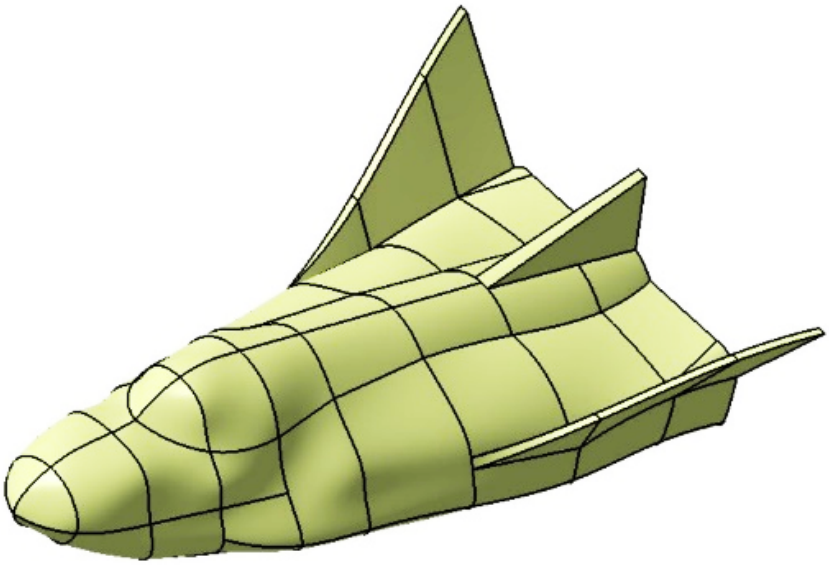

Figure 4.5: Stitched Surface Model

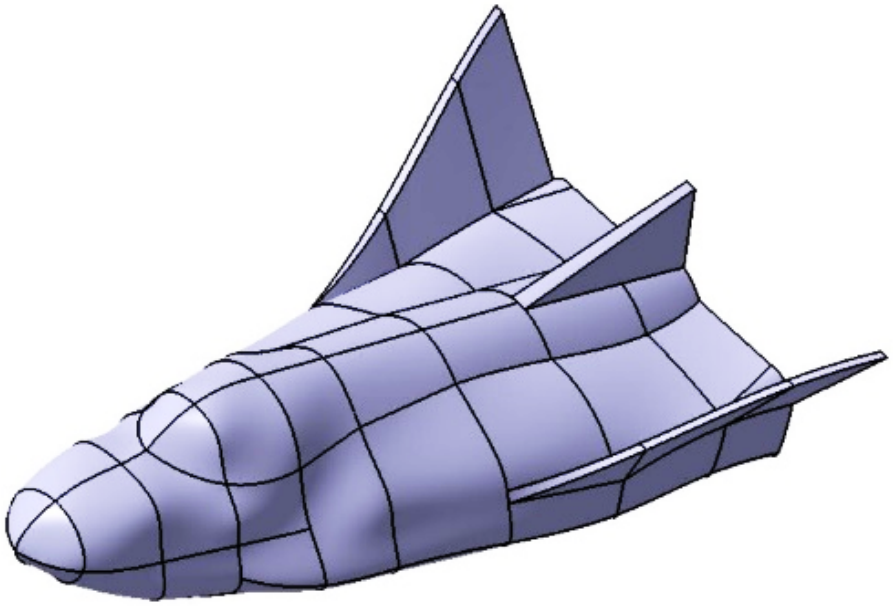

Figure 4.6: Generated Solid Model

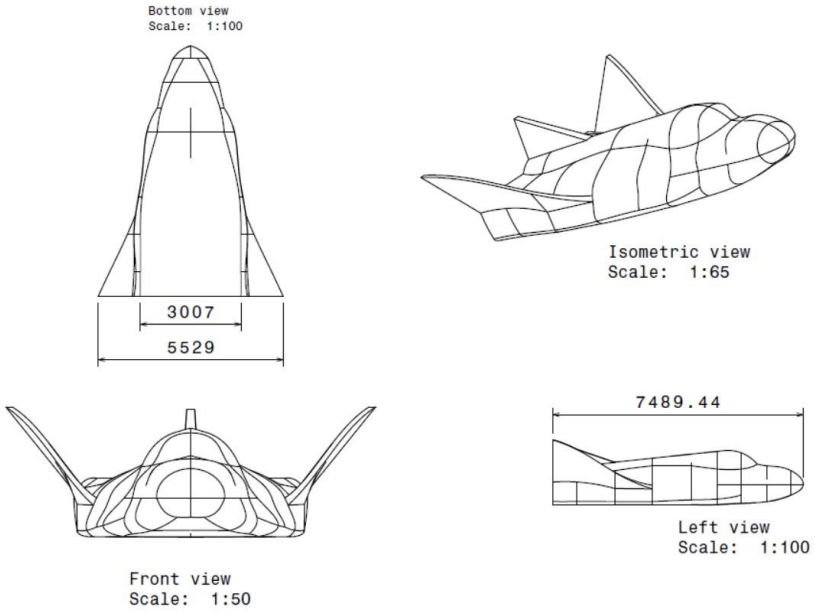

Figure 4.7: HL-20 Original Configuration

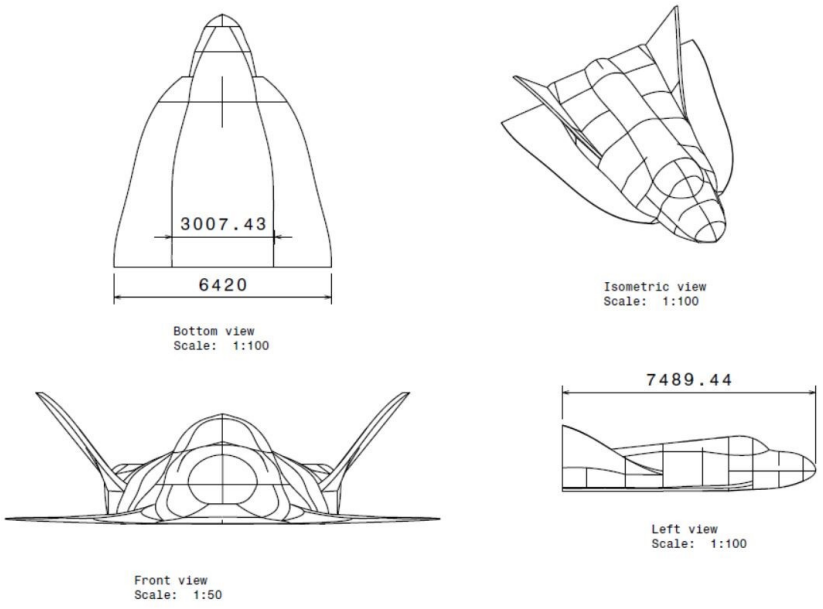

Figure 4.8: HL-20 Modified Configuration with Wing Extension

The meshing and flow simulation over both the models were performed using ANSYS software. The details of the mesh performed and the flow simulation conditions are discussed below.

Grid Size: The grid is an enclosure of 27.5x22x13.2 cuboid, a model symmetric about its longitudinal axis is used to reduce the number of cells and computation time. Due to computational limitations, a grid of larger size couldn't be employed

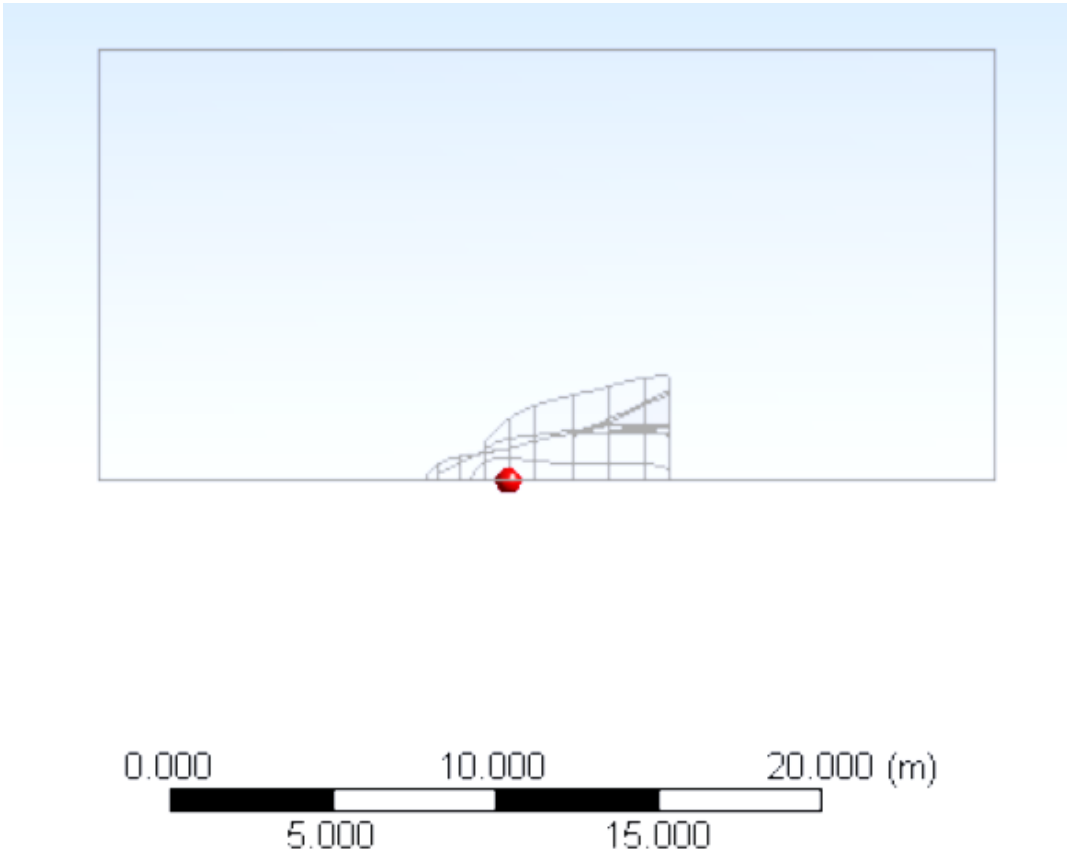

Figure 4.9: Top View of the Grid

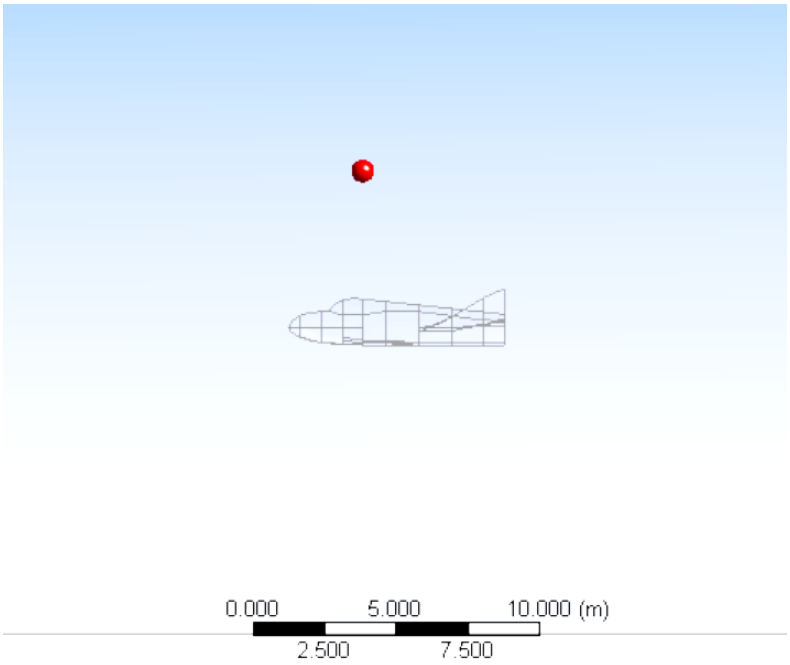

Figure 4.10: Side View of the Grid

Mesh: A static mesh with an average element size of 10cm on the surface of HL-20 and 25 cm on the grid was used. The boundary of the model consists of 10 inflation layers with distance between the nodes being as low as 0.4735 cm.

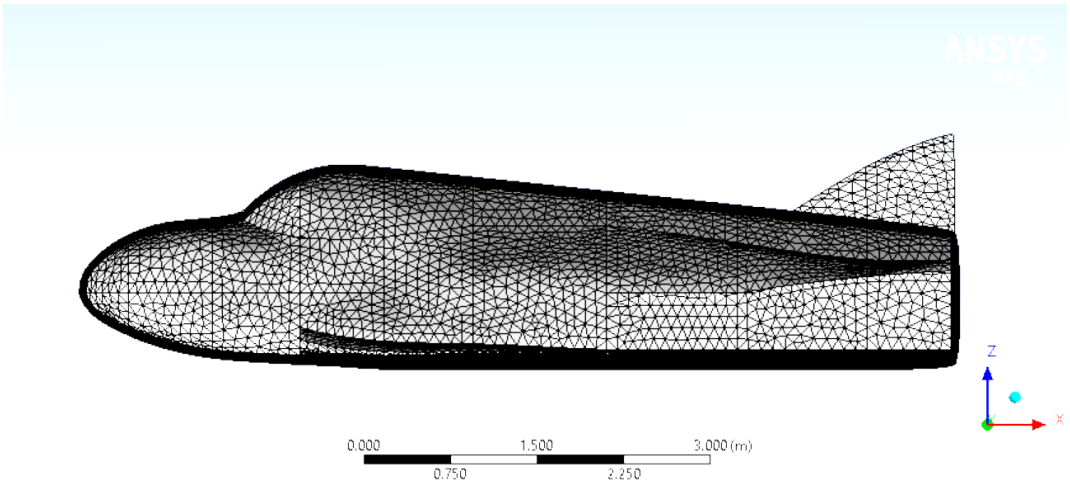

Figure 4.11: Static Mesh performed on the surface of HL-20 Model

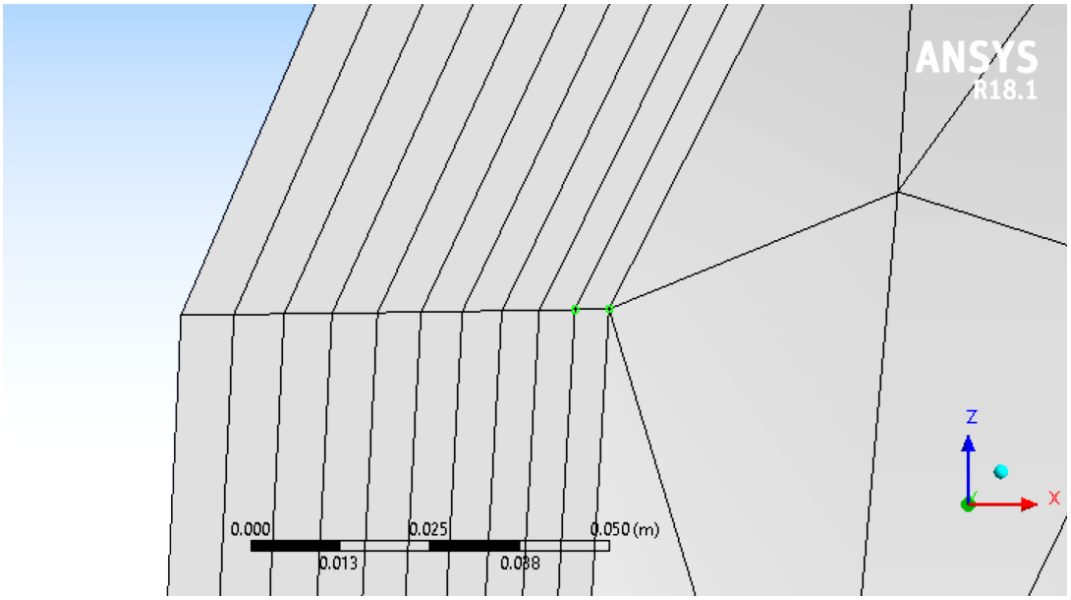

Figure 4.12: Depiction of Minimum Nodal Distance

The Mesh Metric characters like Skewness, Orthogonality, Aspect Ratio and Element Quality employed for the simulation are discussed below.

Skewness: Skewness is a value that measures how much a cell is deformed from its ideal counterpart. For instance, the skewness of an irregular triangle is measured as the deviation of its edges from the corresponding edges of an equilateral triangle. A lower skewness value ensures the regularity of cells. For triangular cells, the skewness value is recommended to be placed below 0.85 in ANSYS for minimizing the computational errors. The mesh employed has a skewness value of cells below 0.65.

Orthogonal Quality: It gives a measure of how close are the angles between the adjacent element faces with respect to an optimal angle. A value close to 1 is recommended for accurate results. The average value of the orthogonal quality of the model was found to be 0.78.

Aspect Ratio: Aspect ratio is the measure of the stretching of a cell. It is defined as ratio of the shortest edge to the longest edge of a cell. ANSYS recommends an average value between 1 to 5 for accurate results. The mesh was found to have an average value of 2.21.

The flow conditions for the simulation was set to match the free-stream atmospheric conditions at an altitude of 60 Km. The flow Mach number was set to M=4.
Ideal compressible gas was used with Sutherland's model to compute the dynamic viscosity. The specific heats were kept constant to reduce the complexities in simulation. With reference to a study made by Miroslav P. Pajcin et al on numerical analysis of hypersonic turbulent and laminar flow, the Standard k- Turbulence model was used for the simulation. The simulations were performed for angles of attack ranging from -5 degree to 35 degree in steps of 5 degrees.

Geometry	**Flow Condition**
Inlet	Mach 4
Outlet	Free-stream conditions
HL-20 Surface	No-Slip Condition
Plane of Symmetry	Symmetry

Figure 4.13: Flow conditions at the interior and exterior of geometry

Mach	4
Altitude (km)	60
Temperature (K)	247.02
Pressure (Pa)	21.96
Density (kg/m^3)	3.10E-04
Dynamic Viscosity (Pas)	1.58E-05

Figure 4.14: Flow properties at 60 km altitude

5

Results and Discussions

The lift coefficients and drag coefficients obtained at different angles of attack are listed in the figure 5.1 for both the configurations.

It is observed that the lift coefficient increases by a fair amount in the configuration

	Original Configuration			Modified Configuration		
Angle of Attack (degree)	Cl	Cd	L/D	Cl	Cd	L/D
-5	-0.7637	0.9959	-0.7669	-1.6505	1.1315	-1.4587
0	-0.0816	0.8958	-0.0911	-0.0861	0.8056	-0.1069
5	0.59797	0.9397	0.6363	0.9552	1.114	0.8575
10	1.3093	1.1264	1.1624	2.2627	1.4694	1.5399
15	2.081	1.4729	1.4129	3.5504	2.0443	1.7367
20	2.4078	1.8385	1.3097	4.9002	2.6936	1.8192
25	2.4464	2.1071	1.1610	4.2978	3.1408	1.3684
30	2.2628	2.2582	1.0020	3.2718	3.526	0.9279
35	1.8074	2.7562	0.6558	2.7855	2.9814	0.9343

Figure 5.1: Lift & Drag coefficients at different angle of attacks

with wing extension as expected. However, it is also accompanied by an early stall occurring at 20-degree angle of attack in the modified configuration. The original HL-20 configuration exhibits a more gradual stall character. The L/D ratio is also found to be higher in the regime of 5 degree to 25 degree for the modified configuration.

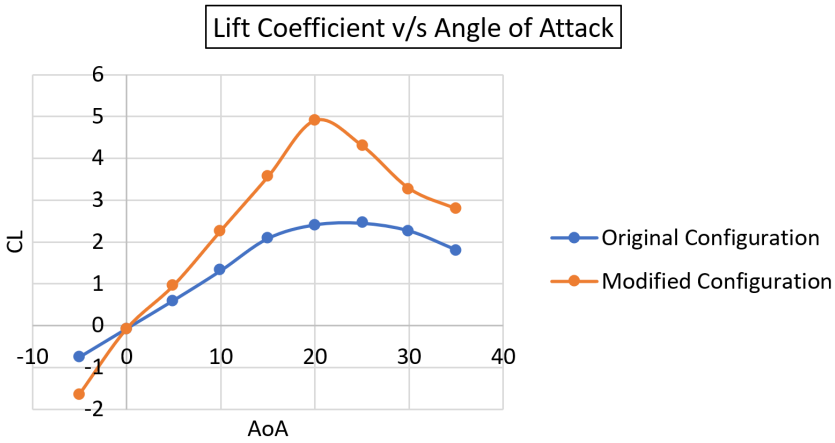

Figure 5.2: Lift coefficient vs Angle of Attack (AOA)

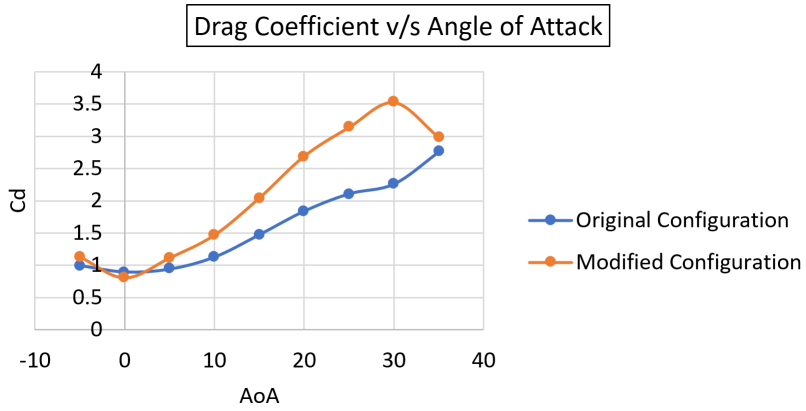

Figure 5.3: Drag coefficient vs Angle of Attack (AOA)

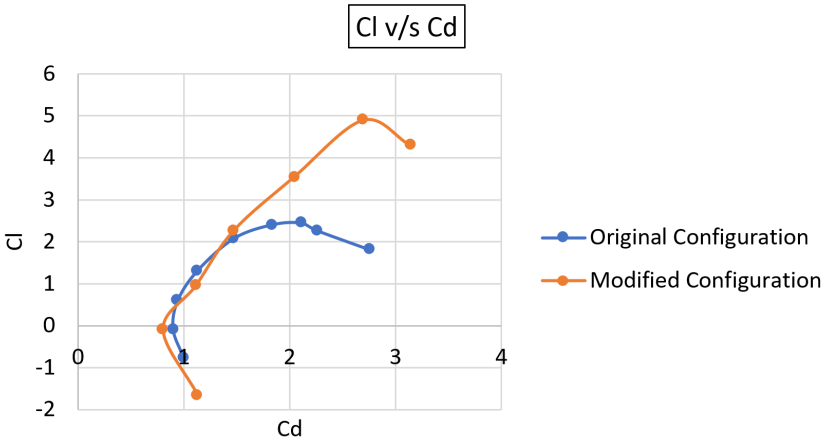

Figure 5.4: C_L vs C_D

6

Conclusions

The re-entry performance of a Lifting Body is determined mainly by its ballistic coefficient and L/D characteristics. A non-lifting body re-entry vehicle like a capsule usually employs a high ballistic coefficient and prefers a direct re-entry trajectory with steeper flight path angles and shorter re-entry time. They result in very high surface heating and limited manoeuvrability. The employment of lift generated and low ballistic coefficient during re-entry in a lifting body configuration results in better re-entry performance. The constraint imposed by the diameter of a launch vehicle on the width of the re-entry vehicle could be overcome by having retractable wing extensions. The increased surface area during re-entry with this modification is valuable in lowering the ballistic coefficient of the vehicle.

Incorporation of wing extensions on the lifting re-entry vehicle showed to induce an early stall performance. However, it was also found to improve the aerodynamic lift and L/D ratio characteristics of the re-entry vehicle. A more precise study on the shape of wing extension has to be made in order to delay the stall and achieve better performance in all flight regimes.

6.1 | Future Work

The current work crudely tries to explore the effects of incorporating a retractable wing extension on HL-20 PLS vehicle. Due to the limitations in the mathematical models

used for simulation in ANSYS software, the study was performed at a lower altitude of 60 km to compare the performances of the designs. There is also a requirement for looking into the mesh size quality and performing the grid independency test to ensure accurate results. A further extension of this work is to explore an optimal wing shape and associated dimensions that result in best aero-thermodynamic performance of the vehicle under all flight regimes ranging from subsonic to hypersonic.

References

[1] Richard M. Wood and Steven X. S. Bauer, 'Flying Wings/ Flying Fuselages', https://www.researchgate.net/publication/23826642, AIAA, 2001

[2] B. Spencer Jr. et al, 'A Study to Determine Methods of Improving the Subsonic Performance of A Proposed Personnel Launch System (PLS) Concept', NASA Technical Memorandum 110201, NASA Langley Research Center, 1995

[3] George M. Ware and Christopher I. Cruz, 'Aerodynamic Characteristics of the HL-20', Journal of Spacecraft and Rockets, Vol. 30, No.5, September-October 1993

[4] Zachary R. Putnam et al, 'Variable Angle-of-Attack Profile Entry Guidance for a Crewed Lifting Body', AIAA

[5] K. James Weilmuenster and Francis A. Greene, 'HL-20 Computational Fluid Dynamics Analysis', Journal of Spacecraft and Rockets, Vol. 30, No.5, September-October 1993

[6] Zhoujie Lyu and Joaquim R. R. A. Martins, 'Aerodynamic Design Optimization Studies of a Blended-Wing-Body Aircraft', DOI: 10.2514/1.C032491, Journal of Aircraft, Vol. 51, No. 5, September-October 2014

[7] Dan Almosnino, 'Assessment of an Inviscid Euler-Adjoint Solver for Prediction of Aerodynamic Characteristics of the NASA HL-20 Lifting Body',

https://www.researchgate.net/publication/303903221, 34th AIAA Applied Aerodynamics Conference, 13-17 June 2016

[8] Yongyuan Li and Yi Jiang, 'Shape Design of Lifting body Based on Genetic Algorithm', http://www.mecs-press.org/, I.J. Information Engineering and Electronic Business, 1, Pg No. 37-43, 2010

[9] G. M. Ware et al, 'Aerodynamic Characteristics of the Hl-20 And Hl-20A Lifting-Body Configurations', https://www.researchgate.net/publication/23856704, AIAA 9th Applied Aerodynamics Conference, September 23-25, 1991

[10] E. Bruce Jackson et al, 'Real-Time Simulation Model of the HL-20 Lifting Body', NASA Langley Research Centre, 1992

[11] Jeffrey S. Robinson and Kathryn E. Wurster, 'Trajectory and Aeroheating Environment Development and Sensitivity Analysis for Capsule-Shaped Vehicles', https://ntrs.nasa.gov/search.jsp?R=20080014105, NASA Langley Research Centre, AIAA, 2008

[12] Soumyo Dutta et al, 'Mission Sizing and Trade Studies for Low Ballistic Coefficient Entry Systems for Venus', https://ntrs.nasa.gov/search.jsp?R=20120006657, IEEE, 2012

[13] 'Reusable Launch Vehicle Programs and Concepts', Associate Administrator for Commercial Space Transportation, 1998

[14] Roger D. Launius and Dennis R. Jenkins, 'Coming Home: Reentry and Recovery from Space', ISBN 978-0-16-091064-7, NASA Aeronautics Book Series, Library of Congress Cataloging-in-Publication Data, 2012

[15] Lane E. Wallace, 'Flights of Discovery', The NASA History Series, Library of Congress Cataloging-in-Publication Data, 1996

[16] R. Dale Reed, 'Wingless Flight: The Lifting Body Story', ISBN 0-16-049390, https://ntrs.nasa.gov/search.jsp?R=19980169231, The NASA History Series, Library of Congress Cataloging-in-Publication Data, 1998

[17] Amanda Deng, 'The Prediction of Aerodynamic Performance and Handling Quality of SpaceShip Two Based on the Analysis of SpaceShip One Flight Test Data', 2012

[18] John C. Adams Jr, 'Atmospheric Re-entry', 2003

[19] Frank W. Taylor et al, 'Challenges and Opportunities Related to Landing the Dream Chaser Reusable Space Vehicle at a Public-Use Airport', Space Traffic Management Conference, Sierra Nevada Corporation, 2014

[20] Sneh Deep and G. Jagadeesh, 'Aerothermodynamic effects of controlled heat release within the hypersonic shock layer around a large angle blunt cone', https://doi.org/10.1063/1.5046191, American Institute of Physics, 2018

[21] Selin Aradag et al, 'Aerodynamic Analysis of a Vertical Landing Lifting Body', ISSN 1300-3615, Journal of Thermal Science and Technology, TIBTD, 2015

[22] Marti Sarigul-Klijn et al, 'Flight Mechanics of Manned Sub-Orbital Reusable Launch Vehicles with Recommendations for Launch and Recovery', https://www.researchgate.net/publication/237448317, AIAA, 2003

[23] Roberta Fusero et al, 'Conceptual design of a crewed reusable space transportation system aimed at parabolic flights: stakeholder analysis, mission concept selection, and spacecraft architecture definition', DOI 10.1007/s12567-016-0131-7, CEAS, 2016

[24] Norman Hahn and Cheryl Perich, 'Active Thermal Control System Radiators for the Dream Chaser Cargo System', 48th International Conference on Environmental Systems, 2018

[25] Erik Seedhouse, 'Tourists In Space: A Practical Guide', ISBN 978-0-387-74643-2, Praxis Publishing Ltd, 2008

[26] Erik Seedhouse, 'Virgin Galactic: The First Ten Years', ISBN 978-3-319-09262-1, Springer International Publishing Switzerland, 2015

[27] Kenneth J. Stroud and David M. Klaus, 'Spacecraft Design Considerations for Piloted Reentry and Landing', https://ntrs.nasa.gov/search.jsp?R=20080026216, 2008

[28] Borg K. and Matula E., 'The SKYLON Spaceplane', University of Colorado, ASEN 5053 – Rocket Propulsion, 2015

[29] S. Tauqeer ul Islam Rizvi et al, 'Optimal trajectory and heat load analysis of different shape lifting reentry vehicles for medium range application', www.sciencedirect.com, Elsevier - Defence Technology 11 (2015) 350e361, 2015

[30] G. Naresh Kumar et al, 'Reentry Trajectory Optimization using Gradient Free Algorithms', www.sciencedirect.com, Elsevier - IFAC PapersOnLine 51-1 (2018) 650–655, 2018

[31] Guo Jie et al, 'Autonomous gliding entry guidance with geographic constraints', Chinese Journal of Aeronautics, (2015), 28(5): 1343–1354. 2015

[32] Miroslav P. Pajcin et al, 'Numerical Analysis of Hypersonic Turbulent and Laminar Flow using a commercial CFD Solver', Thermal Science, Vol.20, Suppl. 6, pp. S1-S13, 2016